Notes

Tangling Effect in Fibrillated Cellulose Reinforced Nanocomposites

My Ahmed Saïd Azizi Samir,[†,‡] Fannie Alloin,[‡] Michel Paillet,[†] and Alain Dufresne*[,§]

Centre de Recherches sur les Macromolécules Végétales (CERMAV-CNRS), Université Joseph Fourier, BP 53, F38041 Grenoble Cedex 9, France; Laboratoire d'Electrochimie et de Physico-chimie des Matériaux et des Interfaces (LEPMI-INPG), BP 75, F38402 St Martin d'Hères, France Cedex; and Ecole Française de Papeterie et des Industries Graphiques (EFPG-INPG), BP 65, F38402, St Martin d'Hères Cedex, France

Received December 18, 2003
Revised Manuscript Received February 13, 2004

Cellulose microfibrils can be found as intertwined microfibrils in the parenchyma cell wall. They consist of cellulose chains stabilized laterally by hydrogen bonds between hydroxyl groups and oxygens of adjacent molecules.[1,2] Depending on their origin, the microfibril diameters range from about 2 to 20 nm for lengths that can reach several tens of microns. They can be extracted from the biomass by a chemical treatment leading to purified cellulose, followed by a mechanical treatment in order to obtain a homogeneous suspension due to the individualization of the microfibrils.[3] They appear as flexible and hairy high aspect ratio fibers. High-performance nanocomposite materials were obtained from cellulose microfibril-reinforced thermoplastics.[4,5]

The microfibrils consist of monocrystalline cellulose domains with the microfibril axis parallel to the cellulose chains. There is also an appreciable amount of cellulose that is in the amorphous state within the microfibril. The crystalline regions in which the linear molecules of cellulose are bonded laterally are characterized by the cellulose lattice which extends over the entire cross section of the microfibril.[6,7] As they are devoid of chain folding and contain only a small number of defects, each microfibril can be considered as a string of polymer whiskers, linked along the microfibril by amorphous domains, and having a high modulus close to that of the perfect crystal of native cellulose (estimated to 150 GPa[8]) and a strength that should be on the order of 10 GPa. The amorphous regions act as structural defects and are responsible for the transverse cleavage of the microfibrils into short nanocrystals under acid hydrolysis.[9,10] Hydrolyzed microfibrils appear as stiff and straight well-defined objects. Since the first announcement of using such whiskers as a cellulosic model reinforcing phase in a polymeric matrix,[11] many works have been published, most of them with tunicin—an animal cellulose.[12−25] The resulting materials display spectacularly enhanced mechanical properties even at a low whiskers content. The formation of a rigid network resulting from strong interactions between adjacent whiskers by hydrogen bonding was proposed to explain the mechanical behavior of cellulose whisker-reinforced composites.

However, no study has been performed to compare the properties of these two cellulosic nanofillers, namely microfibrils and whiskers, and analyze the effect of a progressive acid hydrolysis of the filler on the properties of the composites. In the present work composite materials were obtained from an aqueous suspension of sugar beet cellulose microfibrils and a latex of poly(styrene-*co*-butyl acrylate). The mechanical performances of these materials were analyzed as a function of the hydrolysis level of the filler.

Cellulose microfibrils were extracted from sugar beet as described elsewhere.[3] A chemical treatment consisting of an alkali extraction with a sodium hydroxide (NaOH) solution was performed to solubilize most of the pectins and hemicelluloses. After filtration and rinsing with distilled water, the resulting insoluble residue was bleached with a sodium chlorite ($NaClO_2$) solution. The insoluble bleached cellulosic pulp was suspended in distilled water and homogenized by successive passes through a Manton-Gaulin laboratory homogenizer.

The resulting aqueous suspension (labeled CMF) was used as is or mixed with sulfuric acid. Two acid concentrations in water were used, namely 20 and 60 wt %. The concentration of the acid is the key parameter determining the resulting length of the microfibrils. Hydrolysis was made at 40 °C for 35 min under strong stirring. The suspension was washed with water until neutrality was reached and submitted to a sonication treatment (Branson sonifier). The resulting suspensions were denoted CMF20 and CMF60 for CMF suspensions treated with acid concentrated at 20 and 60 wt %, respectively.

Figure 1 shows TEM micrographs of sugar beet cellulose microfibrils before (CMF, panel a) and after acid hydrolysis (panels b and c). Transmission electron microscopy (TEM) observations were made with a Philips CM200 electron microscope. A droplet of a dilute suspension of fibrillated cellulose was deposited and allowed to dry on a carbon-coated grid. The accelerating voltage was 80 kV. Figure 1a displays well-individualized cellulose microfibrils or still associated together in bundles. Individual microfibrils are almost 5 nm in width and the length is much higher, leading to a practically infinite aspect ratio.

Parts b and c of Figure 1 show TEM micrographs of CMF20 and CMF60, respectively. It is observed that both the length and the diameter of the microfibrils decrease as the concentration of acid increases. The dimensions of the whiskers CMF60 were averaged on

[†] CERMAV-CNRS.
[‡] LEPMI-INPG.
[§] EFPG-INPG.
* To whom correspondence should be addressed: Tel (+33) 4 76 82 69 95; Fax (+33) 4 76 82 69 33; e-mail Alain.Dufresne@efpg.inpg.fr.

10.1021/ma035939u CCC: $27.50
Published on Web 04/28/2004

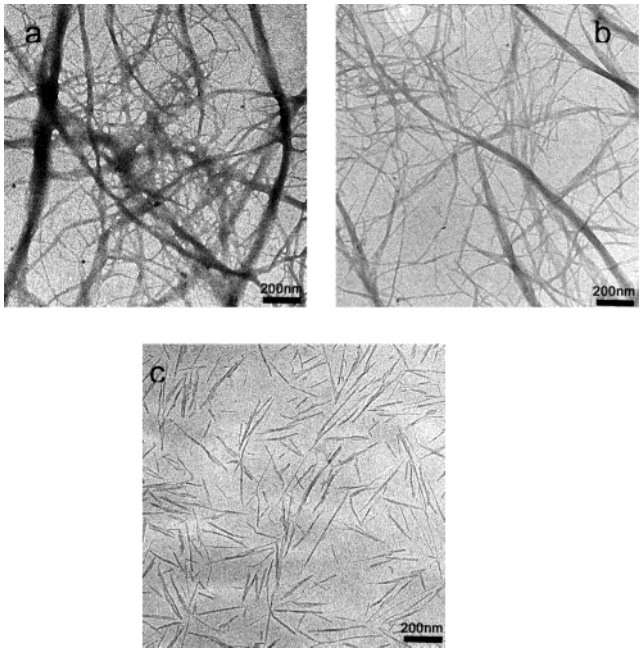

Figure 1. Transmission electron micrographs of a dilute suspension of sugar beet cellulose microfibrils: (a) CMF, (b) CMF20, and (c) CMF60.

30 representative items. The average length was around 210 nm. This is ascribed to the probability of removal of the amorphous material which increases with the concentration of acid. For the strongly hydrolyzed material (panel 1c), most of the amorphous domains are hydrolyzed and rigid whiskers are obtained.

To process nanocomposite materials from cellulose microfibrils aqueous suspensions, with a good level of dispersion, the thermoplastic matrix used was an aqueous suspension of polymer, i.e., a latex. The latex used for the matrix was obtained by the copolymerization of styrene (34% (w/w)) and butyl acrylate (64% (w/w)) and contains 1% acrylic acid and 1% acrylamide. It contained spherical particles with an average diameter around 150 nm and will be referred to as poly(S-*co*-BuA). The glass transition temperature (T_g) of the copolymer was around 0 °C. The choice of this model matrix was justified by its low T_g, allowing film processing by water evaporation at low temperature, and by its fully amorphous nature.

The two aqueous suspensions were mixed and stirred for 24 h at room temperature. Solid films were obtained by casting this suspension on Teflon plates and water evaporation at 40 °C for 1 week. All ensuing composite films contained 6 wt % of cellulose microfibrils and are denoted P6CMF, P6CMF20, and P6CMF60 depending on the concentration of acid used for the hydrolysis step of the filler, P6CMF referring to composite materials reinforced with unhydrolyzed microfibrils.

Dynamic mechanical tests were carried out with a RSA2 spectrometer from Rheometrics working in the tensile mode. The value of 0.05% for the strain magnitude was chosen in order to be in the domain of the linear viscoelasticity of the materials. Measurements were performed in isochronal conditions at 1 Hz, and the temperature was varied between −100 and 250 °C by steps of 3 °C. Figure 2a shows the variation of the storage tensile modulus at 1 Hz as a function of temperature for unfilled poly(S-*co*-BuA) matrix together with composites materials filled with 6 wt % cellulose microfibrils. The behavior of the unfilled matrix (filled

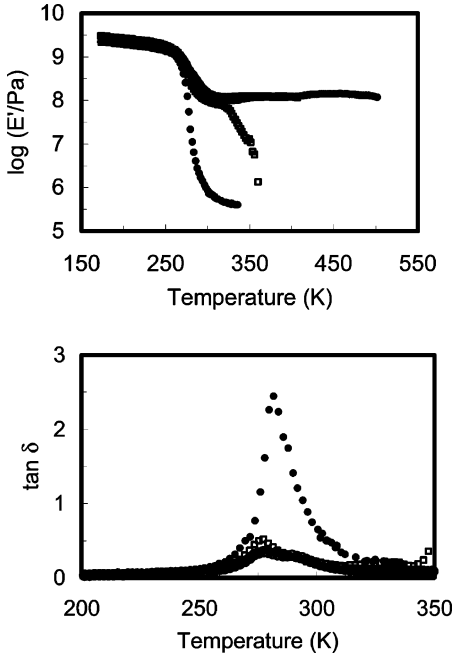

Figure 2. (a) Logarithm of the storage tensile modulus E' and (b) loss angle tangent tan δ vs temperature at 1 Hz for the unfilled poly(S-*co*-BuA) matrix (●) and related composites filled with 6 wt % of sugar beet cellulose microfibrils: P6CMF (○), P6CMF20 (■), and P6CMF60 (□).

circles) is typical of an amorphous thermoplastic. At low temperature, the storage modulus remains roughly constant (∼2−3 GPa) with temperature. Then, a sharp modulus drop corresponding to the glass−rubber transition is observed in the temperature range 270−300 K. This modulus drop corresponds to an energy dissipation phenomenon displayed in the concomitant relaxation process where tan δ passes through a maximum (Figure 2b). At higher temperature, the rubbery material behaves a viscous liquid, and the setup fails to measure the modulus.

For the composite material filled with 6 wt % of unhydrolyzed cellulose microfibrils (P6CMF, open circles), no significant reinforcing effect is reported in the glassy state. On the contrary, the rubbery modulus is strongly increased in the composite compared to the unfilled matrix. For instance, the relaxed modulus at 325 K (around $T_g + 50$ K) is about 240 times higher than that of the matrix. This high reinforcing effect results in a strong decrease of the magnitude of the loss angle for the composite (Figure 2b) and an apparent decrease of the main relaxation process temperature ascribed to a classical coupling effect. In addition to this enhanced mechanical behavior, an increase of the thermal stability of the composite is observed up to 500 K, a temperature at which cellulose starts to degrade. These observations were already reported for cellulose microfibrils extracted from potato pulp and ascribed to the formation of a cellulosic network within the matrix.[4]

For poly(S-*co*-BuA) reinforced with 6 wt % softly hydrolyzed sugar beet cellulose microfibrils (Figure 2, P6CMF20, filled squares), the mechanical behavior is very similar to the one reported for P6CMF. The similitude between the rubbery modulus of both materials is an indication of the similar phenomenon responsible for the high mechanical behavior. Therefore, the reinforcing effect in both systems occurs most probably from the formation of a hydrogen-bonded cellulose network within the matrix. The only significant differ-

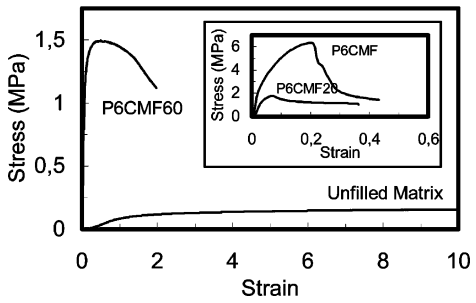

Figure 3. Stress vs strain curves of the unfilled poly(S-*co*-BuA) matrix and related composites filled with 6 wt % of sugar beet cellulose microfibrils. The inset is an expanded view of stress vs strain curves for the most brittle films.

ence between the two composites is the thermal stability of the material, which is much lower (up to about 400 K) for the hydrolyzed filler reinforced polymeric matrix. It could be ascribed from the sole difference between the two kinds of filler that is the flexibility and the resulting possibility of entanglements for unhydrolyzed microfibrils. The higher thermal stability of flexible and hairy microfibrils is therefore ascribed to a tangling effect. However, for tunicin whisker-filled composites the rubbery modulus remained constant up to 500 K.[11,12] The lower thermal stability of hydrolyzed sugar beet cellulose microfibrils could most probably be ascribed to residual pectins at the surface of the filler.[3] The microfibrillar cellulosic network responsible for the high mechanical properties of sugar beet cellulose microfibril-based composites is therefore expected to originate from the formation of interwhisker links through pectins layers. It results in a disastrous decrease of the mechanical properties of the material as soon as the softening temperature of pectins is reached, except if entanglements can keep the cohesion of the cellulosic network.

For the composite material reinforced with strongly hydrolyzed sugar beet cellulose microfibrils (Figure 2, P6CMF60), this tendency is more pronounced, and the modulus drops irreversibly at a temperature very close to the one observed for the unfilled matrix, but more gradually.

The nonlinear mechanical behavior of the composites was analyzed using an Instron 4301 testing machine in the tensile mode. The specimens had the same geometry as those used for the dynamic mechanical tests. The gap between the pneumatic jaws at the starting of each test was adjusted to 15 mm. The stress−strain curves of the samples were obtained at room temperature at a strain rate $d\epsilon/dt = 1.1 \times 10^{-2}$ s^{-1} (cross-head speed = 10 mm min^{-1}). The strain ϵ was determined by $\epsilon = (\Delta L/L_0)$, where ΔL and L_0 were the elongation at the time of the test and the length at zero time, respectively. The stress σ was calculated by $\sigma = F/S_0$, where F was the applied load and S_0 the initial cross-sectional area.

Stress vs strain curves for unfilled poly(S-*co*-BuA) matrix together with composites materials filled with 6 wt % cellulose microfibrils at 25 °C are plotted in Figure 3. At this temperature, the unfilled matrix displays a highly elastic nonlinear behavior typical of elastomeric materials, and the elongation at break was higher by 3000%. The tensile modulus, tensile strength, and elongation at break were determined, and results are collected in Table 1. The tensile or Young's modulus (E) was measured from the slope of the low-strain region.

Table 1. Mechanical Properties of Poly(S-*co*-BuA) Matrix and Related Composites Filled with 6 wt % of Sugar Beet Cellulose Microfibrils

sample	E (MPa)[a]	σ_B (MPa)[b]	ϵ_B (%)[c]
matrix	0.2	0.18	>3000
P6CMF	114	6.3	32
P6CMF20	55	1.7	102
P6CMF60	31	1.5	181

[a] Tensile modulus. [b] Tensile strength. [c] Elongation at break.

It is observed that both the tensile modulus and the tensile strength increase when adding the cellulosic filler, but the reinforcing effect depends on the morphology of the filler. The highest reinforcing effect is reported for the unhydrolyzed microfibril-based composite (P6CMF). As the hydrolysis strength increases, both the modulus and the strength decrease, showing the strong influence of entanglements on the rigidity of the material. The difference between the various samples was not so significant in DMA experiments. This apparent discrepancy could originate from the fact that dynamic mechanical measurements involve weak stresses. The possible interactions between percolating cellulose whiskers are not damaged under these weak stresses. Under the higher stress level, as applied in tensile tests, these interactions seem to be partially destroyed. This is an indication that the residual pectins at the surface of the filler have weakened the strength of the H-bonded cellulose network. It is lower than that of the entangled microfibrils network. The existence and the characterization of residual hemicelluloses at the surface of cellulose microfibrils were reported elsewhere.[26] It was found that around 2% of hemicelluloses were present at the surface.

The elongation at break increases as the strength of the hydrolysis increases. This is an indication that, after destruction of the cellulosic network, the behavior of the composite is mainly governed by the matrix, in agreement with DMA analysis. For the long entangled microfibril-based P6CMF composite the entangled cellulosic network governed the ultimate properties. As the result, the elongation at break decreases.

In conclusion, it appears that the mechanical properties of fibrillated cellulose reinforced nanocomposites can be adjusted by varying the strength of the acid hydrolysis step. One can wonder whether the differences reported between both cellulosic nanofillers could not be ascribed to their different surfaces, the hydrolysis treatment introducing sulfuric groups, whereas residual hemicelluloses are present at the surface of microfibrils. In fact, these two different surface structures are responsible for the stabilization of the aqueous suspensions. They induce differences in the suspension state, but not in the solid state. When the cellulosic fillers are embedded within the polymeric synthetic matrix, these differences do not play any role. This is evidenced by a similar reinforcing effect observed by DMA for both the unhydrolyzed and hydrolyzed filler-based materials in the rubbery state of the matrix. Therefore, entanglements between flexible microfibrils seem to play a crucial part in the mechanical behavior of the nanocomposite, mainly in the nonlinear range.

Acknowledgment. The authors thank the Région Rhône-Alpes for financial support and Mrs I. Pignot-Paintrand for helping in TEM study.

References and Notes

(1) Itoh, T.; Brown, R. M., Jr. *Planta* **1984**, *160*, 372.
(2) Benziman, M.; Haigler, C. H.; Brown, R. M., Jr.; White, A.; Cooper, K. M. *Proc. Natl. Acad. Sci. U.S.A.* **1980**, *77*, 6678.
(3) Dufresne, A.; Cavaillé, J. Y.; Vignon, M. R. *J. Appl. Polym. Sci.* **1997**, *6*, 1185.
(4) Dufresne, A.; Vignon, M. R. *Macromolecules* **1998**, *31*, 2693.
(5) Dufresne, A.; Dupeyre, D.; Vignon, M. R. *J. Appl. Polym. Sci.* **2000**, *76*, 2080.
(6) Marchessault, R. H. In *Cellulose and Wood-Chemistry and Technology*; Schuerch, C., Ed.; Wiley: New York, 1989.
(7) Chanzy, H. In *Cellulose Sources and Exploitation*; Kennedy, J. F., Phillips, G. O., Williams, P. A., Eds.; Ellis Horwood Ltd.: New York, 1990.
(8) Sakurada, I.; Nukushina, Y. *J. Polym. Sci.* **1962**, *57*, 651.
(9) Battista, O. A.; Coppick, S.; Howsmon, J. A.; Morehead, F. F.; Sisson, W. A. *Ind. Eng. Chem.* **1956**, *48*, 333.
(10) Marchessault, R. H.; Morehead, F. F.; Joan Koch, M. *J. Colloid Sci.* **1961**, *16*, 327.
(11) Favier, V.; Canova, G. R.; Cavaillé, J. Y.; Chanzy, H.; Dufresne, A.; Gauthier, C. *Polym. Adv. Technol.* **1995**, *6*, 351.
(12) Favier, V.; Chanzy, H.; Cavaillé, J. Y. *Macromolecules* **1995**, *28*, 6365.
(13) Helbert, W.; Cavaillé, J. Y.; Dufresne, A. *Polym. Compos.* **1996**, *17*, 604.
(14) Hajji, P.; Cavaillé, J. Y.; Favier, V.; Gauthier, C.; Vigier, G. *Polym. Compos.* **1996**, *17*, 612.
(15) Favier, V.; Canova, G. R.; Schrivastava, S. C.; Cavaillé, J. Y. *Polym. Eng. Sci.* **1997**, *37*, 1732.
(16) Dufresne, A.; Cavaillé, J. Y.; Helbert, W. *Polym. Compos.* **1997**, *18*, 198.
(17) Chazeau, L.; Cavaillé, J. Y.; Terech, P. *Polymer* **1999**, *40*, 5333.
(18) Dufresne, A.; Kellerhals, M. B.; Witholt, B. *Macromolecules* **1999**, *32*, 7396.
(19) Chazeau, L.; Paillet, M.; Cavaillé, J. Y. *J. Polym. Sci., Part B: Polym. Phys.* **1999**, *37*, 2151.
(20) Chazeau, L.; Canova, G. R.; Dendievel, R.; Boutherin, B.; Cavaillé, J. Y. *J. Appl. Polym. Sci.* **1999**, *71*, 1797.
(21) Dufresne, A. *Compos. Interfaces* **2000**, *7*, 53.
(22) Matos Ruiz, M.; Cavaillé, J. Y.; Dufresne, A.; Gérard, J. F.; Graillat, C. *Compos. Interfaces* **2000**, *7*, 117.
(23) Anglès, M. N.; Dufresne, A. *Macromolecules* **2000**, *33*, 8344.
(24) Anglès, M. N.; Dufresne, A. *Macromolecules* **2001**, *34*, 2921.
(25) Mathew, A. P.; Dufresne, A. *Biomacromolecules* **2002**, *3*, 609.
(26) Dinand, E.; Vignon, M. R. *Carbohydr. Res.* **2001**, *330*, 285.

MA035939U